

**Bekzod Eshkuvvatov<sup>1</sup>, Bakhtiyor Meliev<sup>2</sup>, Mohammad Suhail<sup>3</sup>, Ibrohim Bekkulov<sup>4</sup>,  
Mekhrison Sharipova<sup>5</sup>, Fatima Zareen<sup>6</sup>**

## **MATHEMATICAL MODELLING OF EROSION PROCESSES IN THE MIDDLE ZARAFSHAN HIGHLAND PLAINS**

### **ABSTRACT**

This article delves into the mathematical modeling of erosion processes affecting the Oktov mountain plains in the Middle Zarafshan Region, a geomorphologically intricate and relatively inaccessible terrain. By utilizing high-resolution satellite imagery, the study aims to enhance the understanding of erosion dynamics in this geomorphologically complex area, where traditional ground-based observations are challenging. Satellite images are processed and analyzed to extract critical data on topographical changes, sediment displacement, and vegetation cover, which are vital indicators of erosion activity. Satellite-derived metrics — such as digital elevation models (DEMs), normalized difference vegetation index (NDVI), and sediment transport estimates — are synthesized to quantify erosion susceptibility. The mathematical models developed in this study are grounded in multivariate geostatistical techniques and erosion prediction equations akin to the Revised Universal Soil Loss Equation (RUSLE), adapted for remote sensing applications. The model employs algorithms that account for various erosive factors such as rainfall intensity, soil composition, slope gradient, and land use practices. The model was validated using ground truthing, ensuring their robustness and accuracy in predicting erosion trends. Through a combination of spatial analysis and numerical simulations, the research identifies the most vulnerable areas to erosion and provides insights into the underlying mechanisms driving these processes. It underscores the significant impact of both natural and anthropogenic factors on the erosion dynamics of the Oktov mountain plains. The findings delineate erosion-prone zones and correlate intensification patterns with both natural gradients and unsustainable agricultural practices, echoing concerns raised in contemporary erosion literature regarding land degradation in semi-arid upland systems.

**KEYWORDS:** erosion modelling, soil and land degradation, sediment displacement, semi-arid uplands, spatial analysis

### **INTRODUCTION**

The importance of cartographic research methods in ensuring the connection of modern geography with mathematics is quite significant. We can see this in the process of data processing when studying events with the help of a map, and defining the problem based on cartographic

---

<sup>1</sup> Samarkand State University named after Sharof Rashidov, Faculty of Geography and Ecology, 15, Universitetsky blvd., Samarkand, 140104, Uzbekistan, *e-mail*: [netgeo.suhail@gmail.com](mailto:netgeo.suhail@gmail.com)

<sup>2</sup> Samarkand State University named after Sharof Rashidov, Faculty of Geography and Ecology, 15, Universitetsky blvd., Samarkand, 140104, Uzbekistan

<sup>3</sup> Samarkand State University named after Sharof Rashidov, Faculty of Geography and Ecology, 15, Universitetsky blvd., Samarkand, 140104, Uzbekistan, *e-mail*: [netgeo.suhail@gmail.com](mailto:netgeo.suhail@gmail.com)

<sup>4</sup> Samarkand State University named after Sharof Rashidov, Faculty of Geography and Ecology, 15, Universitetsky blvd., Samarkand, 140104, Uzbekistan

<sup>5</sup> Samarkand State University named after Sharof Rashidov, Faculty of Geography and Ecology, 15, Universitetsky blvd., Samarkand, 140104, Uzbekistan

<sup>6</sup> Samarkand State University named after Sharof Rashidov, Faculty of Geography and Ecology, 15, Universitetsky blvd., Samarkand, 140104, Uzbekistan

research methods. The existence that surrounds us acts as a primary source of information. When creating cards, the initial data is processed in the registration manager. Here, the primary data is subjected to a complex processing process such as analysis, abstraction, generalization and synthesis [Barnes, 1995; Padma et al., 2024]. The application of mathematics to landscape research is an important issue, as a result of which it is possible to improve the accuracy of maps, to objectify the development of principles of cartographic modeling [Ravshanov et al., 2024]. In the process of using cards in scientific research, the data observed in the next channels of research will be in a new state. This changed data is the result of outgoing data or research. The qualitative and quantitative indicators of the outgoing data depend on the characteristics of the research channel. Therefore, the second important issue in the application of mathematics to landscape research is the search for methods of studying and transforming cartographic images that allow obtaining the desired result as flawlessly as possible [Eshkuvvatov, 2020; Eshkuvvatov et al., 2020; Pasquale et al., 2021].

As we all know, a certain form of surface water erosion occurs on mountain slopes due to rainfall. The work performed by this erosional form is erosive and accumulative, that is, under the influence of gravity, a certain amount of rock is moved from higher to lower places. Hence, the process of erosion takes place. Since the beginning of human farming, the foothills have been the main agricultural land. However, every year, millions of tons of fertile layers are washed away from the erosion plains. Natural erosion processes also occur in areas where irrigated agriculture is not practiced. This study is focused on mathematical modeling based on the analysis of space photographs of pre-mountain erosion plains of the Southern Nurota Range (Middle Zarafshan, southern slope of Oktov). For this purpose, the cosmic image of the erosion plains from the southern foothills of Oktov to the Zarafshan River, where the earth's surface is clearly cut by streams, was taken as a basis. However, creating mathematical models is another important issue in the study of natural territorial complexes [Meliev, 2009; Christine et al., 2019; Meliev, 2019].

At the same time, this issue has attracted the attention of many researchers. But this creates great difficulties. First of all, landscapes are invisible in a very different haze of features, in their dissimilarity. This article addresses the challenges of mathematical modeling of erosion processes in the Middle Zarafshan highlands using satellite imagery and presents the main results of this research. The pioneering quantitative models of erosion networks were first introduced by E. Horton, who established that the amounts and lengths of erosional features of different orders follow a geometric progression, now known as Horton's laws [Horton, 1948]. Subsequent advancements in the mathematical modeling of erosion in plain landscapes were contributed by A. Viktorov and others [Viktorov et al., 2019; Pasquale et al., 2021]. This study builds upon these foundational works, applying contemporary techniques to analyze and predict erosion patterns in the highland regions, offering new insights and confirming the applicability of Horton's principles in a complex geomorphological context [Horton, 1948; Auerswald et al., 2014; Viktorov, 2016].

In general, the use of mathematical methods in landscape research, the use of mathematical models, increases its importance as a practical science, that is, it serves as one of the important tools in the development of various sectors of the economy [Ayres, 1937; Eichorn, 1979; Burrough, 1988; Arnold et al., 1998; Yarashev et al., 2015]. Quantification of landscape zoning is important for different geographical purposes including agriculture, soil, socio-economic landscape, demography, industrial locations, medical geographical zoning and others [Gvozdetsky, 1961; Eichorn, 1979; UNEP, 1979; Le et al., 1996; Blanco-Canqui, Lal, 2008; Suhail, 2023; Ibragimov et al., 2024; Mukhamedov et al., 2024; Ravshanov et al., 2024; Suhail et al., 2024]. This study aims to develop and validate mathematical models for analyzing erosion processes in the pre-mountain erosion plains of the Southern Nurota Range, specifically within the Middle Zarafshan highlands, by leveraging high-resolution satellite imagery and cartographic research methods. It seeks to enhance the integration of mathematics and modern geography through

quantitative landscape modeling, ultimately contributing to improved precision in mapping erosion-prone areas and supporting sustainable land management strategies in geomorphologically complex and agriculturally vulnerable terrains.

## RESEARCH MATERIALS AND METHODS

### Study area

In our study area, erosion plains encompass sloping surfaces and gully-erosion forms with dendritic patterns cut by small rivers and streams in the southern foothills of Oktov (Fig. 1).



*Fig. 1. Typical Satellite image of Oktov erosional plain (Google Earth)*

These surfaces are vegetated variably according to climatic and geomorphological conditions. Oktov, situated in the northern sector of the Middle Zarafshan natural geographical region, is part of the Southern Nurota Ridge [Meliev, 2009; Eshkuvvatov, 2020]. Administratively, it spans the Samarkand and Navoi regions, extending 120 km from southeast to northwest. It is bordered by the Karachitog Ridge to the east, the Kyzylkum Desert to the west, the Nurota Bog to the north, and the Karatog Ridge to the southwest. The average elevation ranges from 1 000 to 1 200 m, decreasing to 600 m in the northwest where it merges with the plain. The highest peak is Takhku, standing at 2003 m. The southern slope of the ridge is notably steeper, incised by numerous rivers and streams. The region's anticlinal structure was formed during the Hercynian orogeny and consists of limestone, shale, and granite, uplifted by Paleozoic tectonic movements. The total area of the mountain is 2 748 km<sup>2</sup>, calculated using space photographs analyzed with ArcGIS software.

### Background of mathematical modelling

Considering the erosional forms on the slopes, the developed erosion processes can be described as a conditional model that means the depressions along the slope merge and form new erosion features. This process eventually leads to the formation of a first-order erosion state (Fig. 2).

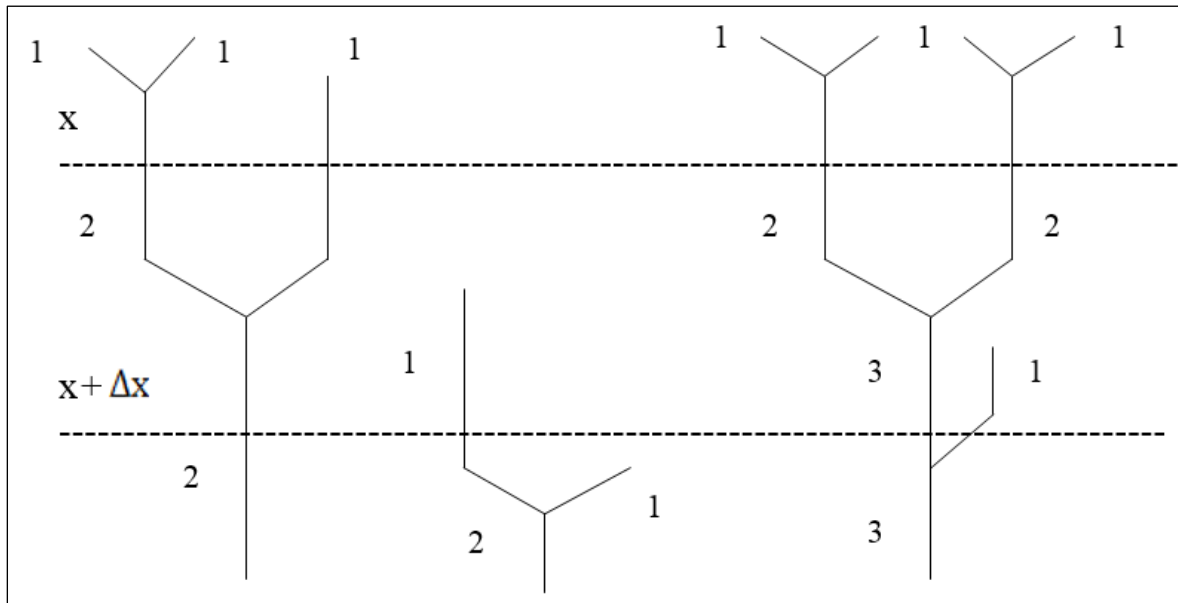


*Fig. 2. Schematic diagram of formation of erosional process (dotted line shows the formation of the boundary, separating upper and lower limit for  $x$  region whereas order stream is represented in their successive order)*

From the figure above, the following main three conclusions can be drawn for mathematical modeling:

- a) The merging of two adjacent erosion forms is independent of the order of other erosion forms. Its probability is directly proportional to the downward movement along the slope, i. e.  $\Delta x$ , and hence the criteria shall be explained as follows (1):

$$\rho_c = \lambda \Delta x + o(\Delta x) \quad (1),$$

where  $\lambda$  is proportionality coefficient.

- b) The emergence of new sources of erosion forms in different areas occurs independently of each other and other erosion forms. Its probability is directly proportional to the size of the area, i. e.  $\Delta S$ , and hence the equation can be written as (2):

$$\rho_c = \lambda_0 \Delta S + o(\Delta S) \quad (2).$$

- c) The emergence of new first-order erosion forms depends on the amount that ensures a permanently dense arrangement of erosion forms.

### **Modelling the erosion processes**

The above connotations are deeply rooted in natural processes and various features affecting erosional processes in the study area. Indeed, the merging of adjacent erosional forms is influenced by geomorphological conditions and geological structures, rather than by the order of the erosional forms themselves. The spatial density of these forms should be such that an erosional form emerges from rainfall. Despite their naturalness and universality, these three conclusions necessitate a detailed examination of the mathematical model of erosion plains to accurately capture the complexity and nuances of these natural processes. Understanding the behavior of erosional forms requires acknowledging that their merging is a result of specific geomorphological and geological conditions, which dictate the pathways and interactions of surface water flow. This

implies that the probability of two adjacent erosional forms merging is inherently linked to the slope gradient, soil composition, and underlying rock structures, rather than simply the hierarchical order of the forms. Moreover, the formation of new sources of erosion in different areas operates independently of existing forms and is directly proportional to the size of the area in question. This independence highlights the stochastic nature of erosion processes, where new erosional forms can develop anywhere based on localized climatic and geological conditions, without being influenced by the presence or configuration of nearby erosional forms [Belyaev et al., 2005]. The creation of first-order erosional forms is also contingent on the amount of precipitation that ensures a densely packed arrangement of these forms. This condition underscores the importance of rainfall intensity and frequency in shaping the landscape, as continuous and heavy rainfall promotes the development of densely spaced erosional features.

Further, in these intricate dynamics, the proposed mathematical model must account for the natural and universal principles governing erosion while also integrating specific geomorphological and geological parameters. This dual approach will enhance the model's accuracy in predicting erosion patterns and behaviors, providing valuable insights for managing and mitigating the impacts of erosion in vulnerable regions. Therefore, as per the eq. 2, the distribution of the number of erosional forms in an arbitrarily selected area must satisfy Poisson's law, and can be written as (3):

$$\rho(k) = \frac{(\lambda_0 S)^k}{k!} e^{-\lambda_0 S} \quad (3),$$

where  $S$  is the size of the experimental area, the average density of the located sources.

The number of convolutions and intermingling of any erosional pattern also obeys Poisson's law (4):

$$p_1(k) = \frac{(\lambda l)^k}{k!} e^{-\lambda l} \quad (4),$$

where is  $\lambda$  — the average density of inclusions of erosional forms,  
 $l$  — cross-section length.

The distribution of distances between adjacent curves corresponds to an exponential distribution (5):

$$F_{\xi}(x) = 1 - e^{-2x} \quad (5).$$

The conclusion about the constancy of the density of erosion networks allows us to find the correlation between the parameters (magnitudes) of the models. Consider a long transect ( $S$ ) parallel to the base of the slope and another similar length ( $\Delta x$ ) below it, where the first transect is crossed by  $N$  erosional features. In it, we can see that the decrease in number due to the merging of erosional forms is compensated by new erosional forms in the area between the transects (6):

$$[\lambda \Delta x + o(\Delta x)]N = \lambda_0 S \Delta x \quad (6).$$

Dividing both sides of the equation by  $\Delta x$ , we get (7):

$$\lambda = \lambda_0 \bar{r}, \quad (7),$$

where  $\bar{r}$  is the average distance between adjacent erosion forms in an arbitrary transect.

We make two  $x$  and  $y$  transects along the slope, which differ from each other in steps. Transects demarcate some fragments. Then, in the lower transect, the share of the main erosional form formed by joining the erosional forms between them is equal to the share of the first-order erosional forms starting in this interval. In this case, (1) can be written as follows:

$$\gamma = \lambda\Delta x + o(\Delta x) \quad (8).$$

Accordingly, the percentage of erosional forms that pass from one transect to another transect without joining is equal to (9):

$$\beta = 1 - 2\lambda\Delta x + o(\Delta x) \quad (9).$$

It is clear from the above that at each new step, the arbitrary order of the component (except for the first one) is formed at the expense of three sources, and following conclusion can be made as:

- 1) a component that has not been combined with any other components in the previous step and has kept its sequence number (organizer);
- 2) a constituent formed by the addition of a constituent of lower order in the previous step, but retaining its sequence number;
- 3) the component  $(i - 1)$  formed by joining two constituents in the previous step and the founder of the first order;
- 4) organizers who did not have a branch in the previous step;
- 5) appropriately included in the system as a condition of model formation.

Thus, the analysis of the formation of the above-mentioned constituents of different orders shows that the development of the system can be expressed in the following equations, taking into account the addition and order of the erosional forms independently (10):

$$\begin{cases} p_i(x + \Delta x) = \beta p_i(x) + \gamma \\ p_i(x + \Delta x) = \beta p_i(x) + 2\gamma p_i(x)[p_i(x) + \dots + p_{i-1}(x)] + \gamma[p_{i-1}(x)]^2 \end{cases} \quad (10).$$

Here, the probability that the constituent of the  $p_{i(x)} - i^{\text{th}}$  order is located at a distance  $x$  from the upper limit of its field. Coefficient 2 in the second equation is set to make it clear that the constituent of the given order can be obtained through another constituent added to it from the right, or through another constituent added from the left exactly similar to it, that is, each pair of constituents to be added can be interchanged. For example, the order of pairs of constituents  $(i, j)$  can be replaced by another order of pairs  $(j, i)$ . Taking into account the equalities in (8) and (9),  $\Delta x \rightarrow 0$  then we have a system of differential equations (11):

$$\frac{dp_i}{dx} = \lambda(1 - 2p_i), \quad \text{or} \quad \frac{dp_i}{dx} = 2\lambda(p_i + \dots + p_{i-1} - 1)p_i + \lambda p_{i-1}^2 \quad (11).$$

Let's look at the equation for the solution of the first function as (12):

$$p_i(x) = \frac{1}{2} (1 - e^{-2\lambda x}), \quad \text{so} \quad \lim_{x \rightarrow \infty} p_i(x) = \frac{1}{2} \quad (12).$$

By applying the method of mathematical induction to the first equation and its constituents, it is possible to prove that the constituents of different orders are likely to aspire in a limited interval. Accordingly, these limits must satisfy the following system (13):

$$1 - 2p_i = 0, \text{ therefore, } 2\lambda(p_i + \dots + p_{i-1} - 1)p_i + \lambda p_{i-1}^2 = 0 \quad (13).$$

Solving the equation, we get (14):

$$p_i = \frac{1}{2}, i = 1, 2, \dots \quad (14).$$

In addition, the equations can be solved as follows (15):

$$p_i \approx \frac{1}{2^i} + \left( p_{i0} - \frac{1}{2^i} \right) e^{\frac{\lambda}{2^{i-2}}(x-x_0)} \quad (\text{where } p_{i0} = p_i(x_0)) \quad (15).$$

## RESEARCH RESULTS AND DISCUSSION

The findings serve as the foundation for the following conclusions, i. e., the probability of erosion features developing on slopes, regardless of their hierarchical order or complexity, tends to stabilize around specific values. This trend appears to hold true irrespective of the likelihood of additional erosional forms being introduced. In essence, the formation of erosion structures follows a predictable pattern, with their occurrence on similar slopes converging toward consistent probabilities, unaffected by the potential for further erosional developments [Borrelli et al., 2013]. The mathematical model of the hypothesized erosion plains allows us to find the numbers of interdependencies of different order components in the system. Let us look at the formation of a system of erosional forms of order  $(k + 1)$ , where the probability of component  $(p_i)$  of different order is outside the system. The ordering of each component in this system begins with the addition of the component to order  $(i - 1)$  (adding a tributary smaller than  $i$  and ending with joining an erosional form of order equal to or greater than  $i$ ). In this case, taking into account the independent combination of different erosion forms, it can be seen that the number of sections in the component distribution corresponds to the geometric distribution (16):

$$p(\xi_i = k) = (p_i + \dots + p_{i-1})^{k-1} [1 - (p_i + \dots + p_{i-1})] \quad (16),$$

where  $p_i \rightarrow i$  is the probability of the tributaries of the order joining each other, where the average value of the fragments is (17):

$$k_i = \frac{1}{1 - (p_i + \dots + p_{i-1})} \quad (17).$$

It is equal to the average value of internal tributaries, which can further be written as (18):

$$n_i^o = \frac{p_i + \dots + p_{i-1}}{1 - (p_i + \dots + p_{i-1})} \quad (18).$$

Applying (eq. 14) for large values of  $x$ , we get (19):

$$p(\xi_i = k) = \frac{1}{2^i} \left( 1 - \frac{1}{2^i} \right)^{k-1} \quad (19).$$

In the component of order  $k$ , we find the value of the distribution of erosion forms of different order  $(i)$  (20, 21):

$$\varphi_{ik}(t) = \sum_{j=0}^{\infty} (p_i + \dots + p_{i-1})^j [1 - (p_i + \dots + p_{k-1})] [1 + p(e^{it} - 1)] \quad (20),$$

now,

$$p = \frac{p_i}{p_i + \dots + p_{k-1}} \quad (21).$$

From this, taking into account the correspondence of the rows, we have the following (22):

$$\varphi_{ik}(t) = \frac{1 - q_i}{1 - q_i e^{it}} \quad (22).$$

Therefore, in the component of the order  $k$ , the parameters of the value of the erosion form of the order  $i$ -th have a geometric distribution (23):

$$q_i = \frac{p_i}{1 - (p_i + \dots + p_{k-1}) + p_i} \quad (23).$$

Further, the average values of the erosion forms of order  $i$ , respectively, can be written as (24):

$$n_{ik}^o = \frac{p_i}{1 - (p_i + \dots + p_{k-1})} \quad (24).$$

Then, in this model, at large values of  $x$  can be explained as (25):

$$\lim_{n \rightarrow \infty} n_{ik}^o = 2^{k-1-i} \quad (25).$$

Accordingly, taking into account two mutually additive constituents for tributaries of order  $(k - 1)$ , we get (26):

$$n_{k-1, k^2} n_{k-1, k}^o, \quad k + 2 \rightarrow 3, \quad x \rightarrow +\infty \quad (26).$$

The proposed mathematical model of the erosion planes allows us to find the values of the relationships of the different order constituents in the system. If  $m_n$  is the number of tributaries, the system accepts  $m$ -order constituents, then, considering the independent addition of tributaries of different orders, the average values of the addition of  $i$ -order constituents (27):

$$n_{ik}^o = N_m \frac{p_i}{p_1 + p_2 + \dots + p_{m-1}} \quad (27).$$

When finding the total values of the constituents in the erosion model, it can be obtained as (28):

$$n_i = 2n_{i+1} + N_{i+1} \frac{p_i}{p_1 + \dots + p_i} + N_{i+2} \frac{p_i}{p_1 + \dots + p_{i+1}} + N_{k+1} \frac{p_i}{p_1 + \dots + p_k} \quad (28).$$

Further solving, it can be obtained as (29):

$$n_i = 2_{i+1} + n_{i+1}n_{i+1}^o \frac{p_i}{p_1 + \dots + p_i} + (n_{i+1} - 2n_{i+2}) \frac{p_i}{p_{i+1}} \quad (29),$$

(from eq. 20), and (30):

$$n_i = 2_{i+1} + n_{i+1} \frac{p_i}{1 + (p_1 + \dots + p_i)} + (n_{i+1} - 2n_{i+2}) \frac{p_i}{p_{i+1}} \quad (30).$$

Now, this equation was developed to generate a function for large values of  $x$ , where the conditions of (eq. 14) are true (31):

$$n_i = 5n_{i+1} - 4n_{i+2} \quad (31).$$

From this, we derive the formula for the total values of  $i$ -order constituents in the  $(k + 1)$  — order system, which is as follows (32):

$$n_i = \frac{4}{3}(n_k - n_{k+1})4^{k-i} - \frac{1}{3}(n_k - 4n_{k+1}), i < k \quad (32).$$

If the system consists of a single constituent of higher order, the expression simplifies to (33):

$$n_i = \frac{8}{3}4^{k-i} - \frac{1}{3} \quad (33).$$

Thus, the average values of the constituents of different orders in the system are somewhat closer to the 4th order geometric progression. The number of fragments of the  $i$ -order constituent also has a geometric distribution, and its average value forms a 2-sign geometric progression. Based on this mathematical model, it is easy to find the distribution of the projections of the organizers of different orders relative to the axis (in the direction oblique to the  $x$ -axis).

As long as the distribution of projections meets the law of exponentiality, then the general projection of the constituents takes arbitrary values of the segments along the length distribution and has the characteristic function, which was developed as (34):

$$\varphi_i(t) = \sum_{k=1}^{\infty} [1 - (p_1 + \dots + p_{i-1})](p_1 + \dots + p_{i-1})^{k-1} \left(\frac{l_1}{l_1 - it}\right)^k \quad (34),$$

where  $l_1$  — the average length of the segment projection, which was solved as (35):

$$\varphi_i(t) = \frac{l_1}{l_1 - it} \quad (35).$$

For this,  $l_1$  — the average length of the component, of course the length of the components, the equation shall obey the exponential law.

The average length of the components is found from Wald's similarity theory, and it is further developed as (36):

$$l_i = l_1 2^{i-1} \quad (36).$$

As a result, it forms a geometric progression with two denominators. The model provides an analytical solution to the problem of the number of erosional forms crossing an arbitrary cut-off section taken parallel to the base of the slope (Fig. 3, left & right). Let  $S$  be the length of an arbitrary section parallel to the base of the slope, separated by  $x$ , and  $p_{ij}(\Delta x)$  is the number of parallel bases that differ from each other by  $\Delta x$  when the number of initial intersections is equal to  $i$ , the probability of events equal to  $j$   $p_{ij}(\Delta x)$   $x$  will not depend on  $x$ , since it occurs independently of one another. Hence, the number of intersections in the specified slices can be considered as a continuous time as explained in Markov's process;  $p_{ij}(\Delta x)$  is its migration probability, and  $p_i(x)$  is the probability of the number of intersections in the segment  $i$ , located  $x$  above it. The Markov's parameters can be used where  $\lambda_{ij}$  — is the density of transition from  $i$  to  $j$  of intersecting erosion forms.

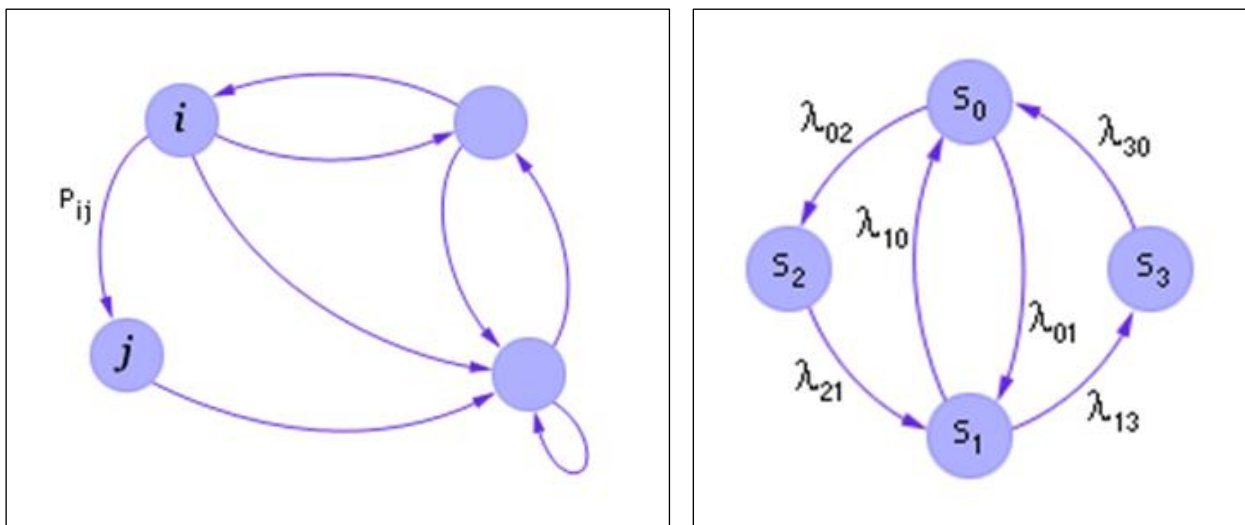


Fig. 3. Designations:  $i$  to  $j$  transition model (left), variation model of inter-field source density (right)

It was observed that the probability of displacement is influenced by the presence of erosion patterns, where the  $i$ -th erosion pattern cuts through the upper slice ( $i \neq 0$ ) and the  $i + 1$  erosion pattern affects the lower slice. In this context, considering the non-merging of erosional forms between fragments and the emergence of a new source, along with the application of equality, the following conditions arise.

$$p_{i,i+1}(x) = \lambda_o s \Delta x + o(\Delta x), i = 1, 2, \dots \quad (37).$$

These observations highlight the dynamics of erosion processes, shaped by the interaction of successive erosion patterns and the distinct separation of erosional forms across different layers. If, in the upper section, the  $i$ -th erosion pattern corresponds to the lower erosion form ( $i - 1$ ), it indicates that no new erosion form has developed between these sections, and instead, the two erosion forms have merged. This observation suggests that the interaction between the sections leads to a unification of the existing erosion patterns, rather than the formation of additional erosional features. Consequently, the merging process between these forms governs the evolution of the erosion structure across the sections. Therefore, the following conclusions can be drawn.

$$p_{i,i-1}(x) = i \lambda \Delta x + o(\Delta x), i = 1, 2, \dots \quad (38).$$

From this, we deduce that  $j \neq i \pm 1$ , meaning that the index  $j$  does not immediately precede or follow  $i$ . This implies a distinct separation between these erosion forms, where no direct adjacent interaction occurs between the  $i$ -th and  $j$ -th erosion patterns. Consequently, this condition reflects the absence of immediate merging or influence between neighboring erosion features, allowing for a clearer distinction between their respective behaviors (Fig. 4).

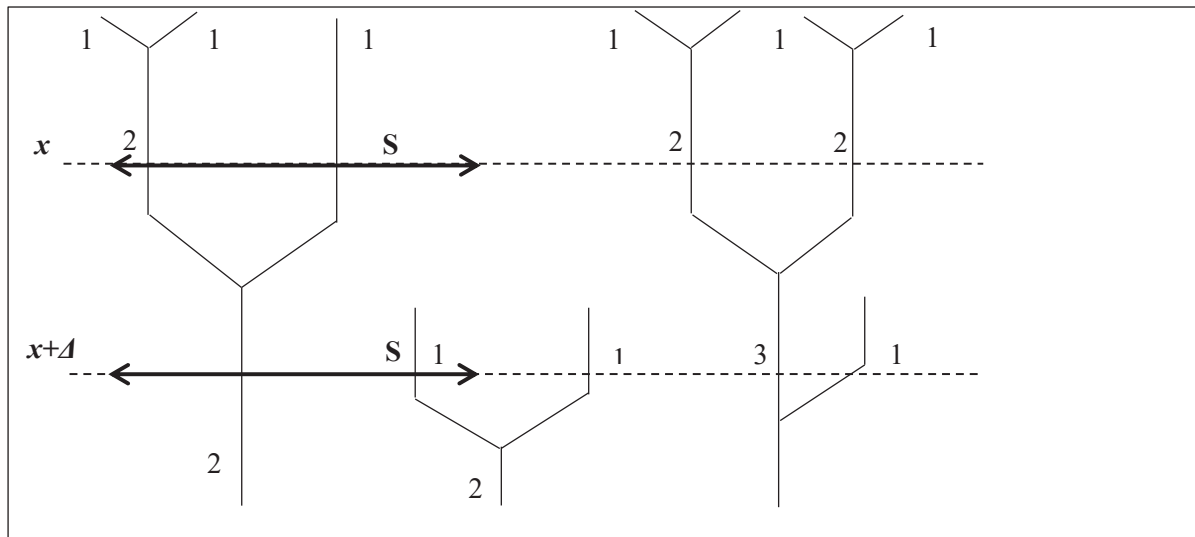


Fig. 3. Intersections of erosional forms with random transects and distribution law scheme of the number (  $\longleftrightarrow$  — transect slices,  $S$  — piece length, ----- — location of the transect on slopes, ——— — schematic representation of natural complexes (landscape) of erosional origin)

To validate the mathematical models of erosion plains, a comprehensive base plot was generated using satellite imagery of erosion plains with proluvial deposits located in the foothills of Oktov. This region is characterized as a foothill plain primarily composed of loess formations, with sections where bedrock surfaces are exposed. The bedrock consists of Paleozoic shales and granitic intrusions that emerge sporadically. The sections observed in the spatial images represent highly fragmented erosion planes, featuring prominent slopes and intricate surface disruptions. In order to conduct the necessary tests, satellite images of the base site were obtained from the Landsat space station on two separate dates: May 3, 2019, and May 9, 2022. The initial step involved automatically calculating and mapping the Normalized Difference Vegetation Index (NDVI) for each set of images, which provides a quantifiable measure of vegetation density and health across the landscape [DeJong et al., 1994; DeVente et al., 2005].

Further, a differential map was generated to capture and visually represent the dynamics of interannual changes between the two periods. This map enabled a clear comparison of vegetation changes over time, highlighting variations in land cover and environmental conditions across the base site. The methodology provided a robust framework for assessing the temporal shifts in vegetation patterns and their potential implications for erosion and landform stability. In this analysis, the number of erosion sources in the base plots was determined using the Poisson distribution, with calculations performed through the Microsoft Excel program. This statistical approach was applied to ensure accuracy in estimating the frequency of erosion events across the study area. Following these calculations, critical values were computed at significance levels of 0.95 and 0.99 to compare the empirical data against the theoretical framework of Pearson's distribution (Table 1, Fig. 4–6).

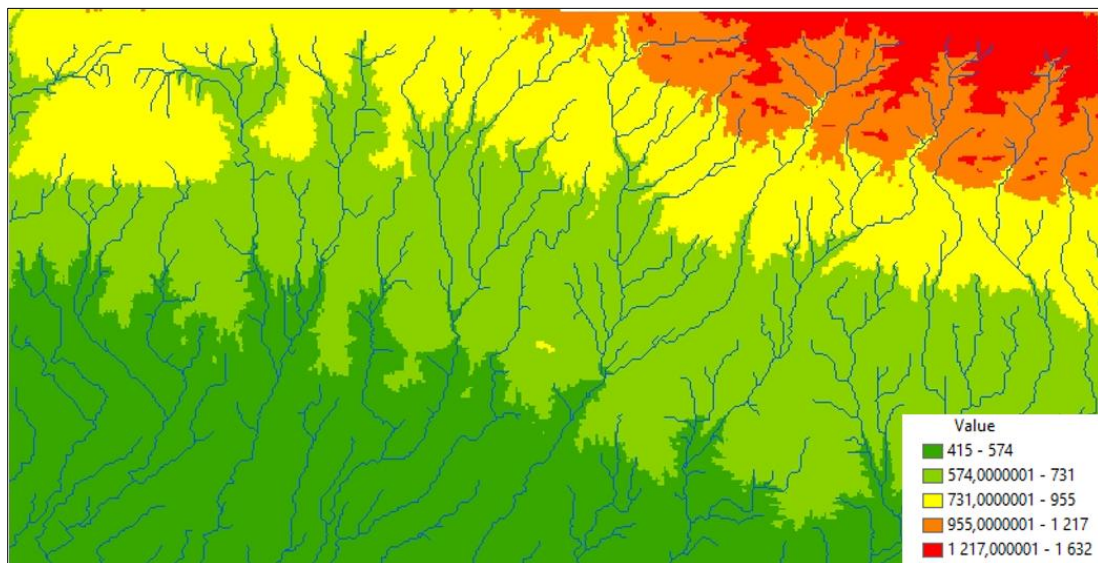


Fig. 4. Prognostic map of the zone of formation of erosion forms of the base section (Oktov)

Table 1. Poisson distribution and the results of the number of sources in the erosion network

Characteristics of the plot	Plot No.	Field size, ha	Average size, $\mu$ m	$\chi^2$	$\chi^2_{0,95}$
Loess highland plains of Oktov with a large slope	1	2000	0,42	0,866	3,841
		4000	0,82	1,536	5,991
		6000	1,17	6,043	7,815
		8000	1,44	6,266	7,815
		10000	1,97	19,23	9,488

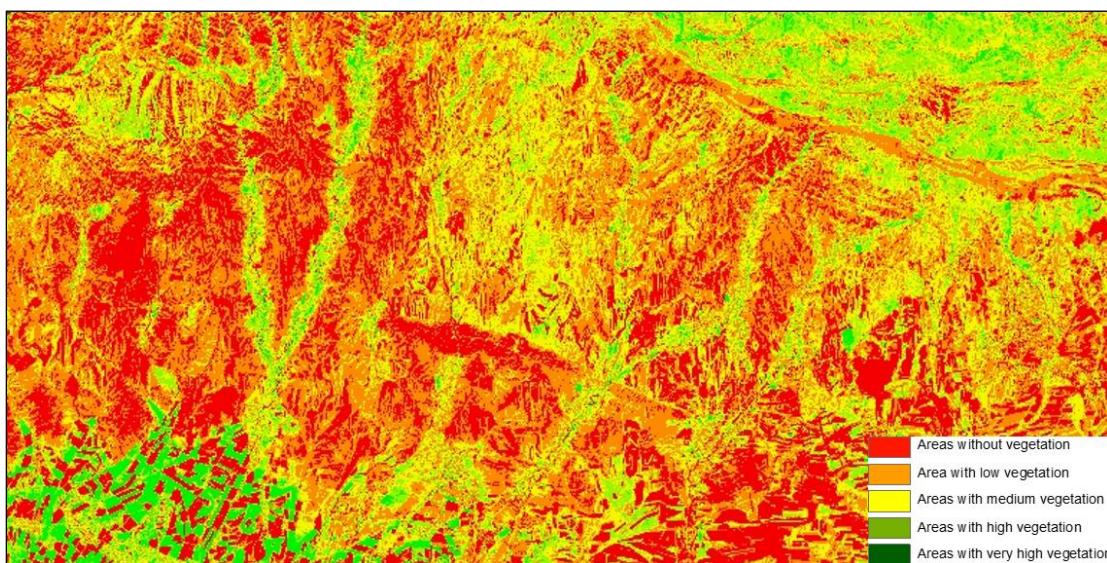
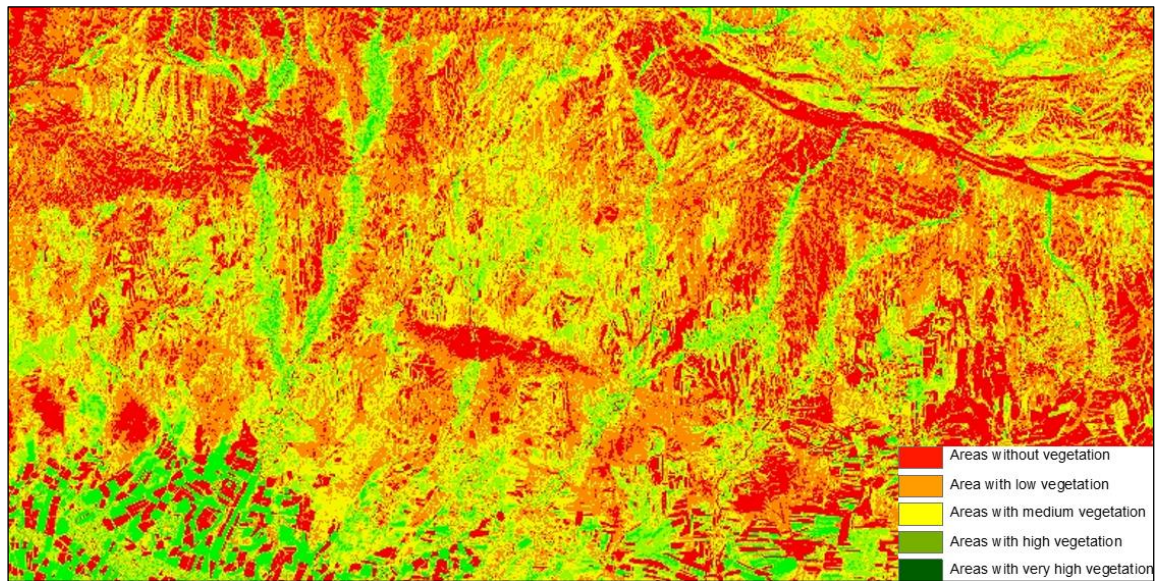


Fig. 5. NDVI analysis of the satellite image taken on May 3, 2019

*of the researched base section in Middle Zarafshon (Oktov)*



*Fig. 6. NDVI analysis of the satellite image taken on May 3, 2023  
of the researched base section in Middle Zarafshon (Oktov)*

This comparison provided a rigorous basis for evaluating the alignment of observed erosion patterns with the predictions of the mathematical models. Through this method, the robustness and reliability of the proposed models were systematically tested, enhancing our understanding of erosion dynamics in this geologically complex region.

## CONCLUSIONS

This study utilized the synthesis of cartographic and mathematical abstraction in geomorphology, demonstrating their symbiotic capacity to decode erosion dynamics in highland agro-ecological systems. Building on Horton's laws [Horton, 1948] and Viktorov's planar landscape models [Viktorov, 2016], the research transcends prior biome-specific limitations by adapting stochastic frameworks — notably Poisson-distributed spatial densities and Markovian process dynamics — to the heterogeneities of the Southern Nurota Range. The validation of geometric progressions in erosional feature lengths (Eq. 36) and exponential decay in inter-feature distances (Eq. 5) aligns with Wald's similarity theory, corroborating deterministic regularities within stochastic erosional systems. Critically, the model's predictive fidelity, tested via NDVI differential mapping and Pearson's distributional thresholds (Fig. 4–6), addresses a lacuna in highland erosion literature, which has historically prioritized qualitative over quantitative cartographic synthesis. The stabilization of erosion probabilities (Eq. 19) and hierarchical independence of merging events (Eq. 37–38) challenge assumptions of erosional determinism in slope systems, echoing Eichhorn's (1979) advocacy for probabilistic geomorphology. However, the model's reliance on static  $\lambda$  coefficients (Eq. 1–2) mirrors critiques by [Yarashev et al., 2015], who emphasize the need to integrate anthropogenic drivers and climatic stochasticity — a limitation this study partially mitigates through interannual NDVI temporal analysis. By operationalizing Horton's principles in a fragmented, loess-dominated highland (Fig. 1–3), the research bridges theoretical geomorphology and applied land stewardship. The geometric progression of tributary lengths (Eq. 33) offers a scalable metric for soil-loss forecasting, while the Poisson-driven erosion-source distribution (Eq. 3) refines UNEP (1979) frameworks for vulnerable agro-zones. Future

iterations must incorporate dynamic feedbacks between vegetation decay and erosional intensity — a gap underscored by [Ravshanov et al., 2024] — to enhance predictive granularity. Finally, this work reaffirms mathematics as the cornerstone of modern cartography, enabling precision in both abstraction (e. g., ArcGIS-derived spatial calibrations) and application (e. g., erosion mitigation). As anthropogenic pressures escalate, such interdisciplinary synergy is not merely advantageous but imperative for reconciling ecological resilience with agrarian viability.

## REFERENCES

- Arnold J. G., Srinivasan R., Muttiah R. S., Williams J. R.* Large Area Hydrologic Modeling and Assessment. Part I: Model Development. *Journal of the American Water Resources Association*, 1998. V. 34. No. 1. P. 73–89.
- Auerswald K., Fiener P., Martin W., Elhaus D.* Use and Misuse of the K Factor Equation in Soil Erosion Modeling: An Alternative Equation for Determining USLE Nomograph Soil Erodibility Values. *CATENA*, 2014. V. 118. P. 220–225. DOI: 10.1016/j.catena.2014.01.008.
- Ayres Q. C.* Soil Erosion and its Control. *Soil Science*, 1937. V. 43. No. 5. P. 391.
- Barnes G.* Land and Geographic Information Systems. *The Surveying Handbook*. Boston, MA: Springer, 1995. DOI: 10.1007/978-1-4615-2067-2\_35.
- Belyaev V. R., Wallbrink P. J., Golosov V. N., Murray A. S., Sidorchuk A. Y.* A Comparison of Methods for Evaluating Soil Redistribution in the Severely Eroded Stavropol Region, Southern European Russia. *Geomorphology*, 2005. V. 65. No. 3–4. P. 173–193.
- Blanco-Canqui H., Lal R.* Principles of Soil Conservation and Management. Springer Science & Business Media, 2008.
- Borrelli P., Robinson D. A., Fleischer L. R., Lugato E., Ballabio C., Alewell C., Meusburger K., Modugno S., Schütt B., Ferro V., Bagarello V.* An Assessment of the Global Impact of 21<sup>st</sup> Century Land Use Change on Soil Erosion. *Nature communications*, 2017. V. 8. No. 1. P. 2013.
- Burrough P. A.* Principal of Geographical Information Systems for Land Resources Assessment. Oxford: Clarendon Press, 1988. 194 p.
- Christine A., Pasquale B., Katrin M., Panos P.* Using the USLE: Chances, Challenges and Limitations of Soil Erosion Modelling. *International Soil and Water Conservation Research*, 2019. V. 7. Iss. 3. P. 203–225. DOI: 10.1016/j.iswcr.2019.05.004.
- DeJong S. M.* Derivation of Vegetative Variables from a Landsat TM Image for Modelling Soil Erosion. *Earth Surface Processes and Landforms*, 1994. V. 19. No. 2. P. 165–178.
- DeVente J., Poesen J.* Predicting Soil Erosion and Sediment Yield at the Basin Scale: Scale Issues and Semi-Quantitative Models. *Earth-science reviews*, 2005. V. 71. No. 1–2. P. 95–125.
- Eichhorn G.* Land Information Systems: Invited Papers and Discussions During the Symposium of the Federation Internationale Des Géomètres. October 16–21, 1978, Technical University of Darmstadt. Technical University, 1979.
- Eshkuvvatov B. B.* Microzoning and Economic Assessment of Foothills and Propagated Landscape Complexes (by the example of Middle Zarafshan). Author's abstract of dissertation. Samarkand, 2020.
- Eshkuvvatov B. B., Yarashev K. S.* Scientific and Practical Measures of Analysis of Plains and Landscapes. Marsland Press: Nature and Science, 2020. V. 18(3). P. 60–62.
- Gvozdetsky N. A.* Landscape Map as a Basis for Physical-Geographical Zoning (Using the Example of the Syr Darya Region of the Inner and Central Tien Shan). Riga: Scientific Papers of University of Latvia, 1961. V. 37. P. 93–100.

- Horton E.* Erosion Development of Rivers and Drainage Basins, 1948. 158 p.
- Ibragimov L., Sherxolov O., Musayev B., Boboyev S., Sobirova M., Boratova G.* Industrial Development and Assessment of its Impact in Samarkand Region — a GIS Mapping-Based Study. E3S Web of Conferences (EDP Sciences), 2024. V. 590. P. 06002.
- LeBas C., Jamagne M.* Soil Databases to Support Sustainable Development. Joint Research Center (IRSA), 1996. 149 p.
- McEntyre J. G.* Land Information Systems. Springer, Boston, MA: The Surveying Handbook, 1987. DOI: 10.1007/978-1-4757-1188-2\_35.
- Meliev B. A.* Issues of Studying the Landscapes of the Zarafshan Basin Based on Space Data and Mapping Them. Scientific and Theoretical Foundations of Creating the National Atlas of Uzbekistan. Tashkent, 2009.
- Meliev B. A.* Use of Aerospace, Mathematical and Geoinformation Methods in the Research of Middle Zarafshan Landscapes. Author's abstract of dissertation. Samarkand, 2019.
- Mukhamedov O., Usmanov M., Sattarov A.* Model of Birth Rate in Uzbekistan and its Geographical Aspects. AIP Conference Proceedings, 2024. No. 3147(1).
- Padma V. V. L., Suhail M., Ibragimov L., Sodiye B.* A Comparative Study of Three Supervised Algorithms for Mixed Crop Classification. 6<sup>th</sup> Annual International Scientific Conference on Geoinformatics — GI 2024: “Sustainable Geospatial Solutions for a Changing World”. E3S Web of Conferences, 2024. V. 590. P. 01004. DOI: 10.1051/e3sconf/202459001004.
- Pasquale B., Christine A., Pablo A., Jamil A. A. A., Jantiene B.* et al. Soil Erosion Modelling: A Global Review and Statistical Analysis. Science of The Total Environment, 2021. V. 780. P. 146494. DOI: 10.1016/j.scitotenv.2021.146494.
- Ravshanov A. X., Suhail M., Komilova K., Ravshanov S.* Medical Geographical Zoning in Part of Uzbekistan — A Regional Synthesis. Regional Science Policy & Practice, 2024. V. 16. No. 12. P. 100142. DOI: 10.1016/j.rspp.2024.100142.
- Suhail M.* Assessment of Water Footprint Under Wheat Cultivation in Purvanchal Uttar Pradesh, Northern India. Environment Development and Sustainability, 2023. V. 26. P. 24957–24969. DOI: 10.1007/s10668-023-03665-4.
- Suhail M., Khan M. N., Ravshanov A. X., Usmanov M.* Suitability Assessment of Wind Energy Farming in the Desert Landscape of Zarafshan Valley, Uzbekistan. InterCarto. InterGIS, 2024. V. 30. Part 1. P. 179–192. DOI: 10.35595/2414-9179-2024-1-30.
- UNEP. GIS awareness in agricultural research. Environment Information and Assessment Tech, 1997. 946 p.
- Viktorov A. S., Kapralova V. N., Arkhipova M. V.* Dynamic Modeling for the Morphological Pattern of Thermokarst Plains with Fluvial Erosion on the Base of Remote Sensing Data. Earth Research from Space, 2019. No. 2. P. 55–64. DOI: 10.31857/S0205-96142019255-64.
- Victorov A. S., Kapralova V. N., Orlov T. V., Trapeznikova O. N., Arkhipova M. V., Berezin P. V., Zverev A. V., Sadkov S. A., Panchenko E. G.* Mathematical Morphology of Cryolithozone Landscapes. Moscow: RUDN Publishing, 2016. 232 p. (in Russian).
- Yarashev Q., Meliyev B.* Problems of Studying and Mapping Paragenetic Landscape Complexes in Surkhandarya Region. European Sciences review, 2015. V. 3–4. No. 14. P. 7–19.